

# Electronic Structure of the Electron-Poor Dinuclear Organometallic Compounds [(CpM)(CpM')]μ-Cot (M, M' = V, Cr, Fe, Co)

Uwe Richter,<sup>†</sup> Jürgen Heck,<sup>‡</sup> and Joachim Reinhold<sup>\*,†</sup>

Institut für Physikalische und Theoretische Chemie, Universität Leipzig, Augustusplatz 10-11, D-04109 Leipzig, Germany, and Institut für Anorganische und Angewandte Chemie, Universität Hamburg, Martin-Luther-King-Platz 6, D-20146 Hamburg, Germany

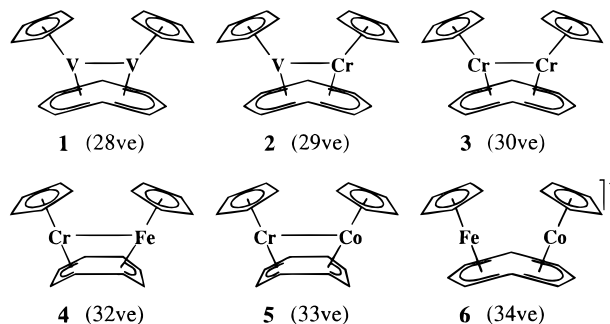
Received May 22, 1998

A systematic theoretical investigation of a variety of synfacial homo- and heterodinuclear organometallic compounds [(CpM)(CpM')]μ-Cot (Cot = cyclooctatetraene; Cp = cyclopentadienyl) is presented. These compounds show, depending on the metals M and M', a number of remarkable and even surprising properties, concerning the metal–metal distances, the magnetic behavior and the spin density distribution. Based on the results of CASSCF calculations, a so-called twinnocene model has been developed, which considers the dinuclear systems as being composed of two separated metallocene-like subunits. The formally nonbonding metal 3d electrons of the subunits interact or do not interact, respectively, in a very specific and characteristic way, to form the dimetal moieties. The model describes the electronic structure, the bonding properties and the wide range of the experimental findings for the whole class of compounds. The strategy followed in the course of the study can be generally recommended for the investigation of dinuclear transition metal complexes.

## Introduction

The nature of metal–metal interactions in dinuclear organometallic compounds is a topic of growing theoretical as well as practical interest, e.g., in the field of catalysis.<sup>1</sup> In the past decade, the Cot-bridged first-row transition metal complexes of the general type [(CpM)(CpM')]μ-Cot (Cot = cyclooctatetraene, Cp = cyclopentadienyl) have been the subject of several experimental and also a few theoretical studies.<sup>2–13</sup> Various homo- and heterodinuclear complexes have been synthesized

Chart 1



and characterized by their structures, NMR and ESR properties and their redox behavior.<sup>2–9</sup> Depending on the metals M and M', a number of remarkable and even surprising properties has appeared. Both, antifacial and synfacial arrangements of the two metal centers with respect to the Cot-ligand have been found. The electron-poor complexes, possessing less than 34 valence electrons (ve), seem to occur exclusively in a synfacial coordination mode (Chart 1), which is considered to be an indication that the electron deficiency at the metal centers is compensated by the formation of direct metal–metal bonds.

For the 28–30ve systems **1–3**, even multiple metal–metal bonds are suggested by electron counting rules. In this way, it appears to be surprising that the intermetallic distance of the formal triple bond in the complex (CpV)<sub>2</sub>μ-Cot is longer or, with respect to the valence radii, at least as long as the formal double bond in (CpCr)<sub>2</sub>μ-Cot (244 vs 239 pm).<sup>2,3</sup> An interesting fact is the variety of magnetic properties within this class of compounds. The (CpV)<sub>2</sub>μ-Cot complex shows a remarkable

<sup>†</sup> Universität Leipzig.

<sup>‡</sup> Universität Hamburg.

- (1) (a) Sinfelt, J. H. *Bimetallic Catalysts: Discovery, Concepts, Applications*; John Wiley: New York, 1983. (b) Hostetler, M. J.; Bergmann, R. G. *J. Am. Chem. Soc.* **1990**, *112*, 8621. (c) Beletskaya, I. P.; Magomedov, G. K.-I.; Voskoboinikov, A. *Z. J. Organomet. Chem.* **1990**, *385*, 289. (d) Esteruelas, M. A.; Garcia, M. P.; López, A. M.; Oro, L. A. *Organometallics* **1991**, *10*, 127. (e) Koo, S. M.; Ryan, D.; Laine, R. M. *Appl. Organomet. Chem.* **1992**, *6*, 437. (f) Rao, Ch. R. K.; Zacharias, P. S. *Polyhedron* **1997**, *16*, 1201. (g) Giordano R.; Sappa, E.; Know, S. A. R. *J. Cluster Sci.* **1996**, *7*, 179. (h) Zhang, Z.-Z.; Xi, H.-P.; Zhao, W.-J.; Jiang, K.-Y.; Wang, R.-J.; Wang, H.-G.; Wu, Y. *J. Organomet. Chem.* **1993**, *454*, 221.
- (2) Elschenbroich, Ch.; Heck, J.; Massa, W.; Nun, E.; Schmidt, R. *J. Am. Chem. Soc.* **1983**, *105*, 2905.
- (3) Elschenbroich, Ch.; Heck, J.; Massa, W.; Schmidt, R. *Angew. Chem.* **1983**, *95*, 319.
- (4) Bachmann, B.; Friedemann, H.; Heck, J.; Wunsch, M. *Organometallics* **1989**, *8*, 2523.
- (5) Bachmann, B.; Baum, G.; Heck, J.; Massa, W.; Ziegler, B. Z. *Naturforsch.* **1990**, *45B*, 221.
- (6) Heck, J.; Rist, G. *J. Organomet. Chem.* **1988**, *342*, 45.
- (7) Heck, J.; Hermans, P. M. J. A.; Scholten, A. B.; Bosman, W. P. J. H.; Meyer, G.; Staffel, T.; Stuermer, R.; Wunsch, M. *Z. Anorg. Chem.* **1992**, *35*, 611.
- (8) (a) Edwin, J.; Geiger, W. E. *J. Am. Chem. Soc.* **1990**, *112*, 7104. (b) Geiger, W. E.; Salzer, A.; von Philipsborn, W.; Piatini, U.; Reingold, A. L. *J. Am. Chem. Soc.* **1990**, *112*, 7113. (c) Froehlich, Ch.; Hoberg, H. *J. Organomet. Chem.* **1981**, *204*, 131. (d) Paulus, E.; Hoppe, W.; Huber, R. *Naturwissenschaften* **1967**, *54*, 67.
- (9) Behrens, U.; Heck, J.; Maters, M.; Frenzen, G.; Roelofsen, A.; Sommerdijk, T. *J. Organomet. Chem.* **1994**, *475*, 233.
- (10) Lüthi, H. P.; Bauschlicher, C. W., Jr. *J. Am. Chem. Soc.* **1987**, *109*, 2046.

(11) Mougnot, P.; Demuyneck, J.; Bénard, M.; Bauschlicher, C. W., Jr. *J. Am. Chem. Soc.* **1988**, *110*, 4503.

(12) Weber, J.; Chermette, H.; Heck, J. *Organometallics* **1989**, *8*, 2544.

(13) Poumbga, Ch.; Daniel, Ch.; Bénard, M. *J. Am. Chem. Soc.* **1991**, *113*, 1090.

temperature-dependent change between dia- and paramagnetism.<sup>4</sup> A triplet state seems to lie only slightly above the singlet ground state and is easily thermally populated. For the analogous diamagnetic (CpCr)<sub>2</sub>μ-Cot system, no such low-lying triplet state exists,<sup>4–6</sup> whereas the complex [(CpCr)(CpFe)]μ-Cot is paramagnetic and contains two unpaired electrons.<sup>7</sup> The spin density distribution is rather surprising, looking at the heterodinuclear open-shell systems [(CpV)(CpCr)]μ-Cot,<sup>3</sup> [(CpCr)(CpFe)]μ-Cot, and [(CpCr)(CpCo)]μ-Cot.<sup>7</sup> The unpaired electrons are not delocalized between the two metal centers, but have been found to be strongly localized at the less noble metal center.

The special interest in multiple metal–metal bonds between first transition row atoms as well as the experimental finding of the temperature-dependent change between dia- and paramagnetism have stimulated several quantum chemical investigations of the vanadium system (CpV)<sub>2</sub>μ-Cot (**1**). Lüthi and Bauschlicher (LB) have found that, at the restricted SCF level, the formally V–V triply bonding configuration is not the most stable one.<sup>10</sup> The lowest closed-shell configuration represents a metal–metal single bond, whereas the four remaining 3d electrons are mainly localized at the metal centers. In contradiction to the experiment, they have found that a <sup>3</sup>B<sub>2</sub> configuration is lower in energy than the closed-shell configurations. Mougnot et al. (MDBB) even yielded a <sup>5</sup>A<sub>1</sub> state as the lowest configuration at the restricted SCF level.<sup>11</sup> However, inclusion of the important nondynamical correlation effects by a suitable CI procedure has led to the correct energetic order of the different spin states, <sup>1</sup>A<sub>1</sub> < <sup>3</sup>B<sub>2</sub> < <sup>5</sup>A<sub>1</sub>. It was shown that in the <sup>1</sup>A<sub>1</sub> ground-state all six 3d electrons are involved in metal–metal bonding interactions. The description of the metal–metal interaction in terms of a weak triple bond was corroborated by Weber et al. (WCH) by the results of multiple-scattering Xα calculations.<sup>12</sup> Pombga et al. (PDB) have confirmed these results by using an iterative multireference CI procedure.<sup>13</sup> Complete active space SCF (CASSCF)<sup>14</sup> calculations, which would have been desirable to account for the nondynamical correlation effects, were not possible at that time. It has to be mentioned that the method used by PDB yields CASSCF-like results and even includes some dynamical correlation. However, their method requires a very high computational effort and can hardly be applied to more than only a few systems.

Quantum chemical calculations for any other system of this class of compounds have not been carried out up to now. It is the aim of this paper to present such calculations for a variety of synfacial-coordinated neutral and ionic systems [(CpM)-(CpM')]μ-Cot (see Chart 1). On the basis of the results, a general model has been developed, which is capable to describe the electronic structure and the bonding conditions as well as the magnetic properties and the spin density distribution for the whole class of compounds under study.

### Computational Details

Recent applications have shown that the main features of the electronic structure of transition metal compounds can be described properly by CASSCF wave functions (see e.g. ref 15). To achieve reliable results, the definition of an appropriate active space is an essential requirement. However, for systems

containing weakly bonded metal centers and bridging ligands, it is often not obvious, which molecular orbitals are most important for the description of the nondynamical correlation effects and, therefore, have to be included into the active space. For that reason, we carried out extensive preliminary studies at the RHF, ROHF and UHF levels of theory.

In the treatment of such sizable systems one has to decide whether to consider small model ligands to perform highly accurate calculations or to involve the whole ligand system at the expense of a somewhat lower accuracy. In correspondence to the other authors, who worked on this subject (refs 10–13), we decided for the latter. Therefore, we had to restrict ourselves to comparably small basis sets. Various sets were tested for the parent system (CpV)<sub>2</sub>μ-Cot both for the metal centers and the ligand system. For the metal centers, finally, Ne core ECPs of Hay and Wadt<sup>17</sup> were employed, including the outermost core orbitals (3s,3p) into the variational procedure. The largest ligand basis that could be handled was 6-31G\*\*, yielding 414 contracted basis functions for the system, which is a rather large basis for CASSCF calculations. It turned out, however, that a 3-21G ligand basis (242 contracted functions) leads to almost identical CASSCF results, concerning the natural orbital occupation numbers and the singlet–triplet separation. Therefore, the smaller basis was used throughout the calculations.

The molecular geometries were fitted as exactly as possible to the available experimental data, only slightly modified to achieve perfect C<sub>2v</sub> and C<sub>s</sub> symmetry for the homonuclear and the heteronuclear species, respectively.

For the closed-shell SCF calculations, the Turbomole<sup>18</sup> package was applied. The open-shell SCF and the CASSCF calculations were carried out with the GAUSSIAN<sup>19</sup> system, which provides a direct CASSCF algorithm.

### Results and Discussion

**The 28–30ve Complexes.** Despite of their different formal metal–metal bond order, the complexes **1** and **3** have nearly identical molecular geometries.<sup>2,3</sup> On the other hand, as mentioned in the Introduction, they show a completely different magnetic behavior. In addition, in **3** a fast rotation of the Cot-ligand has been found by <sup>1</sup>H NMR experiments, whereas in **1** the Cot-ring is fixed.<sup>4</sup> These facts make it an attractive task to compare the electronic structures of both systems by means of quantum chemical calculations. We started by calculating the energies of a large number of closed-shell and of some selected open-shell configurations for both systems at the restricted SCF level. The configurations with the lowest energies are summarized in Tables 1 and 2.

For **1**, the energies are referred to the formally V–V triply bonding configuration (...26a<sub>1</sub><sup>2</sup>13a<sub>2</sub><sup>2</sup>16b<sub>1</sub><sup>2</sup>21b<sub>2</sub><sup>2</sup>), where the three bonds are represented by the orbitals 25a<sub>1</sub>, 26a<sub>1</sub>, and 16b<sub>1</sub>. Table 1 shows that not only one substituted closed-shell configuration

- (14) Complete Active Space SCF: (a) Roos, B. O.; Taylor, P. M.; Siegbahn, P. E. M. *Chem. Phys.* **1980**, *48*, 157. (b) Siegbahn, P. E. M.; Almlöf, J.; Heidberg, A.; Roos, B. O. *J. Chem. Phys.* **1981**, *74*, 2384. (c) Roos, B. O. *Int. J. Quantum Chem.* **1980**, *14*, 175.  
 (15) (a) Persson, B. J.; Roos, B. O.; Pierlot, K. *J. Chem. Phys.* **1994**, *101*, 6810. (b) Pierlot, K.; Persson, B. J.; Roos, B. O. *J. Phys. Chem.* **1995**, *99*, 3465. (c) Re, N.; Sgamellottii, A.; Persson, B. J.; Roos, B. O.; Floriani, C. *Organometallics* **1995**, *14*, 63.

- (16) Binkley, J. S.; Pople, J. A.; Hehre, W. J. *J. Am. Chem. Soc.* **1980**, *102*, 939.  
 (17) Hay, P. J.; Wadt, W. R. *J. Chem. Phys.* **1985**, *82*, 299.  
 (18) Ahlrichs, R.; Baer, M.; Baron, H. P.; Ehrig, M.; Haase, F.; Haeser, M.; Horn, H.; Koelmel, C.; Schaefer, A.; Schneider, U.; Weis, P.; Weiss, H. *TURBOMOLE*, Version 3.0(beta); University of Karlsruhe: Germany, 1992.  
 (19) Frisch, M. J.; Trucks, G. W.; Schlegel, H. B.; Gill, P. M. W.; Johnson, B. G.; Robb, M. A.; Cheeseman, J. R.; Keith, T.; Petersson, G. A.; Montgomery, J. A.; Raghavachari, K.; Al-Laham, M. A.; Zakrewski, V. G.; Ortiz, J. V.; Foresman, J. B.; Cioslowski, J.; Stefanov, B. B.; Nanayakkara, A.; Challacombe, M.; Peng, C. Y.; Ayala, P. Y.; Chen, W.; Wong, M. W.; Andres, J. L.; Replogle, E. S.; Gomperts, R.; Martin, R. L.; Fox, D. J.; Binkley, J. S.; Defrees, D. J.; Baker, J.; Stewart, J. P.; Head-Gordon, M.; Gonzales, C.; Pople, J. A. *GAUSSIAN 94*, Revision D.4; Gaussian Inc.: Pittsburgh, PA, 1995.

**Table 1.** Computed Energy Separation of the Low-Lying States at Various Levels of Theory for the Complex (CpV)<sub>2</sub>μ-Cot (**1**)

	state <sup>a</sup>	occupation	ΔE [eV]
RHF	<sup>1</sup> A <sub>1</sub>	...26a <sub>1</sub> <sup>2</sup> 13a <sub>2</sub> <sup>2</sup> 16b <sub>1</sub> <sup>2</sup> 21b <sub>2</sub> <sup>2</sup>	0.00
RHF	<sup>1</sup> A <sub>1</sub>	...25a <sub>1</sub> <sup>2</sup> 14a <sub>2</sub> <sup>2</sup> 16b <sub>1</sub> <sup>2</sup> 21b <sub>2</sub> <sup>2</sup>	-0.60
RHF	<sup>1</sup> A <sub>1</sub>	...26a <sub>1</sub> <sup>2</sup> 13a <sub>2</sub> <sup>2</sup> 15b <sub>1</sub> <sup>2</sup> 22b <sub>2</sub> <sup>2</sup>	-1.45
RHF	<sup>1</sup> A <sub>1</sub>	...25a <sub>1</sub> <sup>2</sup> 13a <sub>2</sub> <sup>2</sup> 16b <sub>1</sub> <sup>2</sup> 22b <sub>2</sub> <sup>2</sup>	-3.13
ROHF	<sup>3</sup> B <sub>2</sub>	...25a <sub>1</sub> <sup>2</sup> 26a <sub>1</sub> <sup>1</sup> 13a <sub>2</sub> <sup>2</sup> 16b <sub>1</sub> <sup>2</sup> 21b <sub>2</sub> <sup>2</sup> 22b <sub>2</sub> <sup>1</sup>	-4.74
UHF <sup>a</sup>	<sup>3</sup> B <sub>2</sub>		-5.24
ROHF	<sup>5</sup> A <sub>1</sub>	...25a <sub>1</sub> <sup>1</sup> 26a <sub>1</sub> <sup>1</sup> 13a <sub>2</sub> <sup>2</sup> 16b <sub>1</sub> <sup>2</sup> 22b <sub>2</sub> <sup>1</sup> 23b <sub>2</sub> <sup>1</sup>	-7.86
UHF <sup>a</sup>	<sup>5</sup> A <sub>1</sub>		-8.99
UHF <sup>a</sup>	<sup>1</sup> A <sub>1</sub>		-9.55
CAS(8/8)	<sup>1</sup> A <sub>1</sub>		-10.36
CAS(8/8)	<sup>3</sup> B <sub>2</sub>		-10.11

<sup>a</sup> For the UHF cases the corresponding RHF notation is used, although the UHF wave functions do not represent pure spin states.

**Table 2.** Computed Energy Separation of the Low-Lying States at Various Levels of Theory for the Complex (CpCr)<sub>2</sub>μ-Cot (**3**)

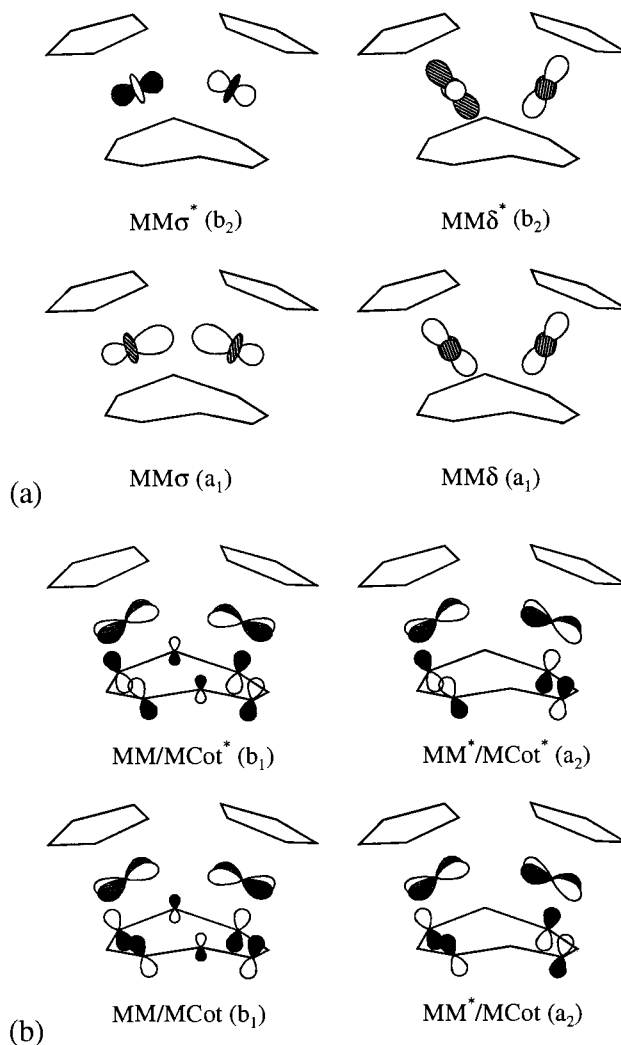
	state <sup>a</sup>	occupation	ΔE [eV]
RHF	<sup>1</sup> A <sub>1</sub>	...26a <sub>1</sub> <sup>2</sup> 13a <sub>2</sub> <sup>2</sup> 16b <sub>1</sub> <sup>2</sup> 22b <sub>2</sub> <sup>2</sup>	0.00
RHF	<sup>1</sup> A <sub>1</sub>	...26a <sub>1</sub> <sup>2</sup> 14a <sub>2</sub> <sup>2</sup> 16b <sub>1</sub> <sup>2</sup> 21b <sub>2</sub> <sup>2</sup>	+5.86
RHF	<sup>1</sup> A <sub>1</sub>	...25a <sub>1</sub> <sup>2</sup> 14a <sub>2</sub> <sup>2</sup> 16b <sub>1</sub> <sup>2</sup> 22b <sub>2</sub> <sup>2</sup>	-0.78
RHF	<sup>1</sup> A <sub>1</sub>	...26a <sub>1</sub> <sup>2</sup> 13a <sub>2</sub> <sup>2</sup> 15b <sub>1</sub> <sup>2</sup> 23b <sub>2</sub> <sup>2</sup>	-1.13
ROHF	<sup>3</sup> B <sub>2</sub>	...26a <sub>1</sub> <sup>1</sup> 13a <sub>2</sub> <sup>2</sup> 16b <sub>1</sub> <sup>2</sup> 23b <sub>2</sub> <sup>1</sup>	-2.58
UHF <sup>a</sup>	<sup>3</sup> B <sub>2</sub>		-3.05
ROHF	<sup>7</sup> A <sub>1</sub>	...25a <sub>1</sub> <sup>1</sup> 26a <sub>1</sub> <sup>1</sup> 27a <sub>1</sub> <sup>1</sup> 13a <sub>2</sub> <sup>2</sup> 16b <sub>1</sub> <sup>2</sup> 22b <sub>2</sub> <sup>1</sup> 23b <sub>2</sub> <sup>1</sup> 24b <sub>2</sub> <sup>1</sup>	-3.24
UHF <sup>a</sup>	<sup>1</sup> A <sub>1</sub>		-4.90
CAS(10/8)	<sup>1</sup> A <sub>1</sub>		-6.06
CAS(10/8)	<sup>3</sup> B <sub>2</sub>		-5.48

<sup>a</sup> For the UHF cases the corresponding RHF notation is used, although the UHF wave functions do not represent pure spin states.

is lower in energy, as it has been pointed out by BL and MDBB, but three different configurations, all of them corresponding to a formal V–V single bond. In agreement with the other authors, the energetic order of the different spin states is <sup>5</sup>A<sub>1</sub> < <sup>3</sup>B<sub>2</sub> < <sup>1</sup>A<sub>1</sub>. For **3**, we refer the energies to the lowest of the formally Cr–Cr doubly bonding configurations (...26a<sub>1</sub><sup>2</sup>13a<sub>2</sub><sup>2</sup>16b<sub>1</sub><sup>2</sup>22b<sub>2</sub><sup>2</sup>). Again, two other closed-shell configurations representing no direct metal–metal bond are lower in energy and the energy decreases with increasing multiplicity, <sup>7</sup>A<sub>1</sub> < <sup>3</sup>B<sub>2</sub> < <sup>1</sup>A<sub>1</sub>. This behavior seems to be somewhat surprising at the first glance, but it is due to the fact that the singlet ground states of these systems cannot be properly described by a closed-shell single determinant wave function, whereas the open-shell states are described more balanced and realistic at this level.

This becomes more clear by looking at the results obtained from the unrestricted SCF calculations. At this level, the energies of the formal singlets decrease considerably, whereas the states of higher multiplicity are only slightly lower than at the restricted level. The energy of the formal singlets is now below the quintet for **1** and the septet for **3**. Nevertheless, the results are yet unsatisfactory, because the higher spin states are not reproduced in the correct sequence. Furthermore, the singlet–triplet separation for **1** appears to be nearly twice as large as for **3**, although no low-lying triplet state has been found for the dichromium system by experiment.

However, the aim of these extensive preliminary investigations was to find out those molecular orbitals, which are important for the description of the near-degeneracy effects. From the character of the MOs of the low-lying restricted configurations (only a few of them are listed in Tables 1 and 2) it has to be concluded that the metal–metal and the relevant metal–Cot–metal interactions essentially involve eight electrons in **1** and 10 electrons in **3**, which are distributed among eight

**Figure 1.** Optimized structure of the active orbitals for (CpV)<sub>2</sub>μ-Cot (**1**) and (CpCr)<sub>2</sub>μ-Cot (**3**): (a) direct metal–metal interactions; (b) metal–Cot–metal and direct metal–metal interactions.

orbitals. These orbitals were defined as active space for the CASSCF calculations of the singlet ground state and the lowest triplet state of both systems. Thus, the active orbital set contains those orbitals, which vary in their occupation within the low-lying restricted configurations. Since this choice is somewhat arbitrary, we additionally determined the natural orbitals for the lowest UHF configurations, as suggested by Pulay and Hamilton.<sup>20</sup> It turned out that the significant partially occupied UHF natural orbitals just correspond to the molecular orbitals selected by means of the low-lying restricted configurations.

Figure 1 shows the optimized structure of the active orbital set. This set can be divided into two subsets. The first (subset a) represents pure direct (through-space) metal–metal interactions and contains the two bonding MOs 25a<sub>1</sub> and 26a<sub>1</sub>, one of essentially σ-bonding character (MMσ), the second mainly of δ-type (MMδ). It is completed by their two antibonding counterparts 22b<sub>2</sub> and 23b<sub>2</sub> (MMσ\* and MMδ\*). The second subset (subset b) essentially constitutes the metal–Cot–metal (metal–metal through-bond) interactions with only small contributions to the direct metal–metal interactions. It contains the two strongly metal–Cot bonding MOs 16b<sub>1</sub> (MM/MCot) and 13a<sub>2</sub> (MM\*/MCot) and their metal–Cot antibonding counterparts 17b<sub>1</sub> (MM/MCot\*) and 14a<sub>2</sub> (MM\*/MCot\*). MO 16b<sub>1</sub>

(20) Pulay, P.; Hamilton, T. P. *J. Chem. Phys.* **1988**, *88*, 4926.



**Table 3.** CAS(8/8) Natural Orbital Occupation Numbers and Dominant Character of the Active Orbitals for the Singlet Ground State and the Low-Lying Triplet State of (CpV)<sub>2</sub>μ-Cot (**1**)

NO	singlet		triplet		character
	occ. no.	M/Cot %	occ. no.	M/Cot %	
17b <sub>1</sub>	0.10	35/64	0.11	34/63	MM/MCot*
14a <sub>2</sub>	0.21	68/28	0.21	69/30	MM*/MCot*
23b <sub>2</sub>	0.47	90/–	0.57	90/–	MMσ*
22b <sub>2</sub>	0.76	94/–	0.95	95/–	MMδ*
26a <sub>1</sub>	1.24	96/–	1.05	94/–	MMδ
25a <sub>1</sub>	1.53	87/–	1.43	90/–	MMσ
16b <sub>1</sub>	1.79	50/47	1.80	47/46	MM/MCot
13a <sub>2</sub>	1.89	33/63	1.88	33/61	MM*/MCot

**Table 4.** CAS(10/8) Natural Orbital Occupation Numbers and Dominant Character of the Active Orbitals for the Singlet Ground State and the Lowest Triplet States of (CpCr)<sub>2</sub>μ-Cot (**3**)

NO	singlet		triplet		character
	occ. no.	M/Cot %	occ. no.	M/Cot %	
17b <sub>1</sub>	0.09	31/65	0.11	29/68	MM/MCot*
14a <sub>2</sub>	0.23	67/33	0.25	75/34	MM*/MCot*
23b <sub>2</sub>	0.42	90/–	1.00	92/–	MMσ*
26a <sub>1</sub>	1.58	89/–	1.00	94/–	MMσ
16b <sub>1</sub>	1.79	63/36	1.78	62/36	MM/MCot
13a <sub>2</sub>	1.89	38/54	1.87	41/53	MM*/MCot
22b <sub>2</sub>	1.99	83/–	1.99	82/–	MMδ*
25a <sub>1</sub>	1.99	85/–	1.99	83/–	MMδ

represents the formal “third” V–V bond, but the 3d–3d overlap within this orbital subset is generally of π/δ type and, for that reason, rather small at the experimental metal–metal distances. Moreover, this weak direct metal–metal bonding interaction is partly compensated due to the metal–metal antibonding character of MO 13a<sub>2</sub>. The importance of subset b is a specific consequence of the electronic structure of the Cot ligand, which is assumed to correspond to that of the planar aromatic Cot<sup>2–</sup> dianion. In this way, orbital 16b<sub>1</sub> (MM/MCot) describes the back-donation from an occupied dimetal orbital into an antibonding ligand π orbital, whereas orbital 13a<sub>2</sub> (MM\*/Cot) describes the strong donation from a formally nonbonding ligand π orbital into an empty dimetal orbital.

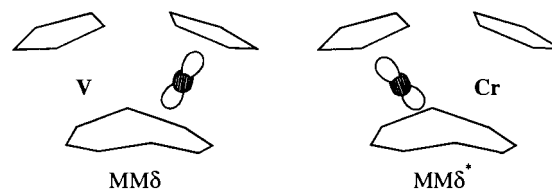
The CASSCF energies are included in Tables 1 and 2. For **1**, a singlet–triplet separation of 23 kJ/mol results, which is in excellent agreement with the experimental value (22–24 kJ/mol).<sup>4</sup> We remark that the results obtained for the vanadium system, in particular the NO occupation numbers, are very similar to those published by PDB.<sup>13</sup> For the chromium system, the calculated singlet–triplet separation is significantly larger (55 kJ/mol), in agreement with the experimental finding, that no low-lying triplet state exists.

The electronic structure of the singlet ground states turns out to be very similar for both complexes. The population of the orbital pair MMσ/MMσ\* is nearly the same (see Tables 3 and 4). This pair represents a moderately strong direct metal–metal σ bond (see Figure 1). The slightly larger occupation number of the σ-bonding MO in **3**, compared to **1**, might be one reason for the fact, that the Cr–Cr distance is shorter than the V–V distance. Very similar effects for both systems also occur in the four orbitals of subset b. The occupation numbers indicate strong metal–Cot bonding interactions. A small difference can only be found in the metal contribution to the orbitals, which again points to a slightly stronger metal–metal bonding interaction in **3**. Consequently, the metal–Cot bonds in **3** should not be as strong as in **1**, which is, in fact, in agreement with the <sup>1</sup>H NMR results, due to which the Cot-ligand is fixed in **1**, but very fast rotating in **3**.

**Table 5.** CAS(9/8) Natural Orbital Occupation Numbers and Character of the Active Orbitals of the Doublet Ground State for the 29ve System (CpV)(CpCr)μ-Cot (**2**)

character	(V–Cr)
MM/MCot*	0.08
MM*/MCot*	0.21
MMσ*	0.40
MMδ* <sup>a</sup>	1.00
MMδ <sup>b</sup>	1.99
MMσ	1.60
MM/MCot	1.80
MM*/MCot	1.91

<sup>a</sup> Localized at the vanadium center (see Chart 2). <sup>b</sup> Localized at the chromium center (see Chart 2).

**Chart 2**

The second orbital pair of subset a, MMδ/MMδ\*, does not have any significant influence on the metal–metal bond, due to the fact that 3dδ interactions are extremely weak at metal–metal distances larger than 200 pm. However, the different number of electrons occupying this pair is responsible for the different specific properties of the two compounds. In **1** the natural orbital populations 1.24/0.76 stand for a relatively strong localization of the two electrons, each at one metal center. The interaction between these two electrons have to be interpreted as weak antiferromagnetic coupling, which is the reason for the temperature-dependent change between the dia- and paramagnetism. In **3**, both orbitals of this pair are doubly occupied and the four electrons have to be considered as two nonbonding electron pairs, each localized at one chromium center. Therefore, in the chromium system, the excitation to the lowest triplet state is not possible within the orbital pair MMδ/MMδ\*, but, as the calculations show, would be connected with the breaking of the Cr–Cr σ bond, which requires a much higher excitation energy.

The heteronuclear system [(CpV)(CpCr)]μ-Cot (**2**) contains 29 valence electrons. ESR experiments have shown that the single unpaired electron is localized at the vanadium center.<sup>4</sup> In the CASSCF calculations for this system the same active space as for **1** and **3** was defined, now correlating nine electrons. Table 5 contains the resulting natural orbital occupation numbers for the doublet ground state.

The structures of the optimized orbitals do not differ significantly from those shown in Figure 1. Again, a direct metal–metal σ-bonding interaction exists, which is indicated by the population of the orbital pair MMσ/MMσ\*. There is also no change, compared to **1** and **3**, in the interplay of metal–metal and metal–Cot interactions within the orbital subset b. The orbital pair MMδ/MMδ\* in **2** is occupied by three electrons. However, no significant influence on the general bonding situation arises from population of this orbital pair, as we have pointed out for the homonuclear species. But, in **2**, the shape of the orbitals of this pair has changed with respect to **1** and **3**, due to the lower symmetry of the system (Chart 2). One orbital is doubly occupied and completely localized at the chromium center. The second orbital contains one single electron and is localized at the vanadium center. Hence, concerning the elec-

Chart 3

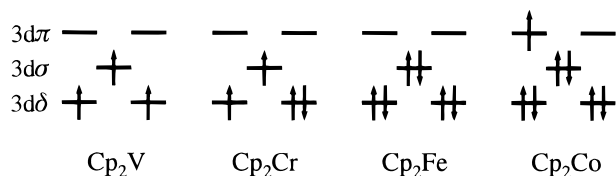
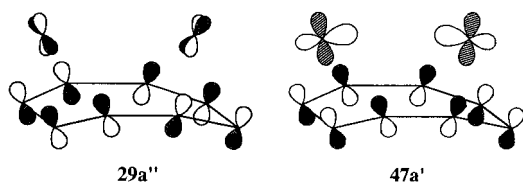


Chart 4



tronic structures of **1** and **3**, the heteronuclear complex can be considered as a fusion of one-half of each of the homonuclear systems.

**The 32–34ve Complexes.** In the heterodinuclear complex [(CpCr)(CpFe)] $\mu$ -Cot (**4**), a metal–Cot  $\eta^4:\eta^4$  coordination mode is realized (see Chart 1), ensuring the same ligand sphere for both metal centers.<sup>7</sup> Formal electron counting leads to a simple valence bond description, where, assuming a metal–metal single bond, 16 and 18 valence electrons are achieved for the chromium and the iron center, respectively. This is corroborated by the intermetallic distance of 272 pm, which is in the range of a Cr–Fe single bond. The molecular structure induced the complex to be considered as a fused chromocene-ferrocene with one carbon atom substituted by a metal atom in each metallocene-like subunit.<sup>7</sup> Therefore, it is suggested that the two unpaired electrons are localized at the chromium center, in correspondence with the electronic structure of chromocene and ferrocene (see Chart 3, which shows the ground-state occupation of the metal 3d orbitals of various metallocenes).<sup>21,22</sup>

We start the discussion of the electronic structure of **4** by subdividing the complex formally into the fragments  $\text{Cp}_2^{2-}$ ,  $\text{Cr}^{2+}$ ,  $\text{Fe}^{2+}$ , and  $\text{Cot}^{2-}$ . Since only very small C–C bond alteration has been found within the Cot ring,<sup>7</sup> the shape of the  $\text{Cot}^{2-}$   $\pi$  orbitals should be similar to the  $\pi$  orbitals of the planar aromatic dianion  $\text{Cot}^{2-}$ . Considering the electronic structure of the metallocenes, the two highest occupied  $\text{Cot}^{2-}$   $\pi$  orbitals should be of special importance. These two orbitals can overlap effectively with empty metal 3d orbitals (Chart 4). Thus, metal–Cot interactions can be expected similar to those found in orbital subset b for the 28–30ve systems. However, if the same metal 3d orbital occupation schemes are realized as in the mononuclear metallocenes, no electrons would remain to form a direct metal–metal bond.

CASSCF calculations should be able to clarify the situation. The definition of an appropriate active space for a proper description of **4** is even more complicated than for the 28–30ve systems. This is due to the fact that the number of active orbitals and electrons, which can be handled, are limited for such large systems. The choice was based on experiences from CASSCF calculations for mononuclear metallocenes. In addition, a number of trial calculations with various active spaces was carried out for **4**. It turned out that the bonding situation is appropriately described by correlating eight electrons within an active space of nine orbitals ( $5a'4a''$ ).

**Table 6.** CAS(8/9) Natural Orbital Occupation Numbers and Character of the Active Orbitals for the Triplet Ground State of (CpCr)(CpFe) $\mu$ -Cot (**4**)<sup>a</sup>

NO	occ. no.	character CpCrCot–CotFeCp
33a''	0.03	ligand
50a'	0.05	4d $\delta$ -lig. $\pi$
32a''	0.05	4d $\delta$ -lig. $\pi$
49a'	0.10	(Cot- $\pi$ $\rightarrow$ Cr-/Fe-3d $\pi$ ) <sup>*</sup>
31a''	1.00	3d $\delta$
48a'	1.00	3d $\sigma$
30a''	1.92	3d $\delta$
47a'	1.92	Cot- $\pi$ $\rightarrow$ Cr-/Fe-3d $\pi$
46a'	1.92	3d $\delta$
inactive (45a')	2.00	3d $\delta$
inactive (44a')	2.00	3d $\sigma$
inactive (29a'')	2.00	Cot- $\pi$ $\rightarrow$ Cr-/Fe-3d $\pi$

<sup>a</sup> The characters are referred to the position of the metal 3d orbitals according to the ligands.

The CAS(8/9) calculations confirm that the ground state of **4** is a triplet. The calculated energy difference between the ground state and the lowest singlet state is 50 kJ/mol. The natural orbital population and the orbital characters for the ground state are given in Table 6. Indeed, it has been found that for both metal centers essentially the metallocene 3d occupation scheme is realized. Three electron pairs are localized at the iron center, one in the inactive orbital 44a' (3d $\sigma$ ), two in the active orbitals 46a' (3d $\delta$ ) and 30a'' (3d $\delta$ ). As in chromocene, the two unpaired electrons are localized at the chromium center. In contrast to the mononuclear compound,<sup>22</sup> in **4**, the unpaired electrons both occupy orbitals of type 3d $\delta$  (48a' and 31a''), while the 3d $\sigma$  orbital (45a', inactive) is doubly occupied. This might be a consequence of the slightly bent structure of the mononuclear subunit or, more general, of the special situation in the dinuclear system.

The orbital 29a'' (inactive) and 47a' represent the two highest occupied  $\text{Cot}^{2-}$   $\pi$  orbitals. A detailed analysis of the orbitals shows that orbital 29a'' is a pure M–Cot–M bridging orbital, describing the donation of electrons into formally empty metal 3d orbitals of both metal centers (see Chart 4). In contrast, orbital 47a' has not merely a pure bridging function. The ligand-to-metal donation induces a weak, but not neglectable, direct metal–metal bonding interaction. This interaction should mainly be responsible for the synfacial structure of the complex.

For the complex [(CpCr)(CpCo)] $\mu$ -Cot (**5**) no structural data are available. For that reason, we adopted for the calculations the same molecular geometry as for **4**. The same nine orbitals were defined as active space. It turns out from the calculations that the general bonding situation is essentially the same in both systems (see Table 7). Three electron pairs are localized at the cobalt center (inactive orbital 44a', active orbitals 30a'' and 46a'), one electron pair (45a') and two unpaired electrons are localized at the chromium center. The additional electron, with respect to **4**, is found to be localized at the cobalt center. As in cobaltocene, it occupies an orbital of 3d $\pi$  character. The shape and the population of the orbitals 31a'' and 32a'' point to a very weak interaction between this additional electron and one of the two unpaired electrons at the chromium center. This interaction has to be interpreted as a weak antiferromagnetic coupling. Thus, in agreement with the experimental results, one unpaired electron remain in the complex, which is localized at the chromium center (orbital 48a'). As in **1**, the weak antiferromagnetic coupling is connected with a very small excitation energy. For **5**, the calculated energy separation between the doublet ground state and the lowest quartet state is even smaller

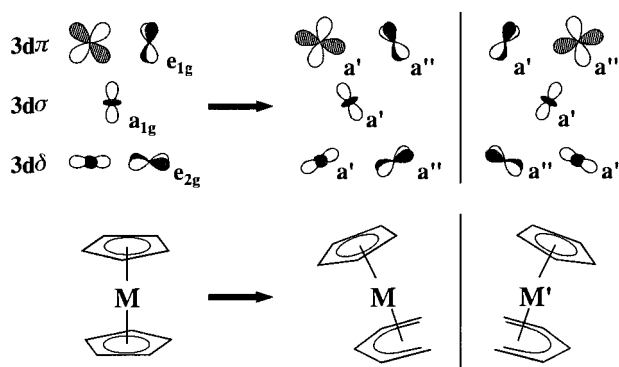
(21) Evans, S.; Green, M. L. H.; Jewitt, B.; Orchard, A. F.; Pygall, C. P. *J. Chem. Soc., Faraday Trans II* **1972**, *68*, 1847.

(22) Evans, S.; Green, M. L. H.; Jewitt, B.; King, G. H.; Orchard, A. F. *J. Chem. Soc., Faraday Trans II* **1974**, *70*, 356.

**Table 7.** CAS(9/9) Natural Orbital Occupation Numbers and Character of the Active Orbitals for the Doublet Ground State of (CpCr)(CpCo) $\mu$ -Cot (**5**)<sup>a</sup>

NO	occ. no.	character CpCrCot—CotCoCp
50a'	0.05	4d $\delta$ -lig. $\pi$
33a''	0.05	4d $\delta$ -lig. $\pi$
49a'	0.13	(Cot- $\pi$ $\rightarrow$ Cr-/Fe-3d $\pi$ ) <sup>*</sup>
32a''	0.89	3d $\delta$ 3d $\pi$
48a'	1.00	3d $\sigma$
31a''	1.11	3d $\delta$ 3d $\pi$
47a'	1.88	Cot- $\pi$ $\rightarrow$ Cr-/Fe-3d $\pi$
30a''	1.93	3d $\delta$
46a'	1.94	3d $\delta$
inactive (45a')	2.00	3d $\delta$
inactive (44a')	2.00	3d $\sigma$
inactive (29a'')	2.00	Cot- $\pi$ $\rightarrow$ Cr-/Fe-3d $\pi$

<sup>a</sup> The characters are referred to the position of the metal 3d orbitals according to the ligands.

**Figure 2.** Orientation and qualitative shape of the metal 3d orbitals in the mononuclear metallocenes and in the dinuclear systems.

than the singlet–triplet separation in **1**. The M–Cot–M interactions indicated by the orbitals 29a'' (inactive) and 47a' are similar to those found for complex **4**. Again, 29a'' is a pure M–Cot–M bridging orbital, whereas a weak direct metal–metal bonding interaction is described by orbital 47a'.

The results of the calculations confirm that complex **4** as well as complex **5** can be considered as being composed of two metallocene-like subunits. The electronic structure of the mononuclear subunits is essentially the same as for chromocene and ferrocene or cobaltocene, respectively. In **4** and **5**, only very weak direct metal–metal bonding interactions occur. These are induced by electron donation from one Cot  $\pi$  orbital into formally unoccupied metal orbitals and do not involve electrons originating from the metal fragments.

In Figure 2 the change of the 3d orbitals is illustrated, going from the mononuclear metallocenes to the subunits of the dinuclear complex. The orbitals undergo merely a rotation by that amount, which put them into a similar position with respect to the ligands as in the mononuclear species. It has to be pointed out that the situation in the 28–30ve systems is very similar, despite only a slight deformation of the metal–metal  $\sigma$ -bonding orbitals.

We note here that, in **5**, a doublet ground state will be realized only for modest metal–metal distances, indicating an antiferromagnetic coupling in this case. Trial calculations for **5** have shown that, at longer intermetallic distances, no interactions exist between unpaired electrons localized at different metal centers. For the latter case, a quartet seems to be the ground state.

In the cationic diamagnetic compound [(CpFe)(CpCo) $\mu$ -Cot]<sup>+</sup> (**6**), the distance of 286 pm between the two metal centers seems to be out of the range of a direct metal–metal bond.<sup>9</sup> The M–C

distances point to a similar coordination mode of the Cot ligand at the metal centers as for the 28–30ve systems (Chart 1). At a first view, it could be assumed that the positive charge is localized at the cobalt center, which would lead to a ferrocene-like metal 3d occupation scheme for both subunits. However, in **6** the charge density at the cobalt center turns out to be the same as in cobaltocene. The resulting Mulliken charges are +0.99 for both metal centers of **6**. This illustrates the function of the ligand system as an effective electron reservoir. The loss of one electron at the cobalt center, with respect to the neutral 35ve system [(CpFe)(CpCo)] $\mu$ -Cot, is completely compensated by donation of electrons from the ligand system. This behavior is comparable to the effect observed for mononuclear complexes as Cp<sub>2</sub>Fe or Cp<sub>2</sub>Co, for which the metal charges remain essentially unaffected, if the systems are oxidized.<sup>23</sup> As expected, a direct metal–metal interaction has not been found. It turned out that the electronic structure of **6**, again, can be discussed in terms of metallocene-like subunits as well.

## Conclusions

**The Twinnocene Model.** A so-called twinnocene model has been introduced originally to predict the localization of the two unpaired electrons at the chromium center in the heterodinuclear complex [(CpCr)(CpFe)] $\mu$ -Cot.<sup>7</sup> The present investigation shows that such a twinnocene model can be applied in a much more general way to describe the properties of the whole class of synfacially coordinated dinuclear first-row transition metal complexes [(CpM)(CpM')] $\mu$ -Cot, including hetero- as well as homodinuclear systems. Each of the compounds can be considered as being composed of two mononuclear metallocene-like subunits. It turned out that the occupation schemes and even the orbital shapes remain essentially the same in the dinuclear complexes, compared to separate metallocenes. Most of the formally nonbonding 3d electrons of the subunits have been found to remain localized at their original metal centers. With respect to the mononuclear metallocenes, no exchange of electrons between the two metal centers of a dinuclear system takes place at all. Thus, electron counting rules, like the 18-electron rule, are not appropriate to describe the bonding schemes of the compounds under study. The metal 3d electrons of the subunits interact or do not interact, respectively, in a very specific and characteristic way to form the dimetal moieties. Direct metal–metal bonds can be expected only in those cases, where both metal centers have unpaired electrons, i.e., in the V–V, V–Cr, Cr–Cr, and Cr–Co systems (**1–3**, **5**). Actually, only in the 28–30ve species one significant direct  $\sigma$ -bonding interaction appears between the two metal centers. On the other hand, in the Cr–Fe and Cr–Co systems (**4**, **5**), a weak metal–metal bonding interaction is induced by electron donation from a strong donating Cot  $\pi$  orbital into the in-phase combination of formally unoccupied metal 3d orbitals. The interactions between the remaining unpaired 3d electrons, being localized at different metal centers, are very weak and have to be interpreted as antiferromagnetic coupling. In the V–V and the Cr–Co system (**1**, **5**), for which such an antiferromagnetic coupling results from the CASSCF calculations, a very small energy separation between different spin states can be predicted, which is known from the experiment for the divanadium system. In addition, formally unpaired metal 3d electrons of the mononuclear metallocene subunits can be involved in metal–Cot bonding interactions, particularly in the 28–30ve species.

(23) Almlöf, J.; Faegri, K., Jr.; Schilling, B. E. R.; Lüthi, H. P. *Chem. Phys. Lett.* **1984**, *106*, 266.

Finally, the spin density distribution and the magnetic behavior can easily be deduced by using the twinnocene model. The number of unpaired spins in the ground state of each dinuclear system is just the difference between the number of unpaired electrons at the two metal centers in the corresponding mononuclear metallocenes. As it has been pointed out, these excess electrons are always localized at their original metal center.

To summarize, the model rationalizes the wide variety of experimental findings of the whole class of compounds under

study. It should be applicable to other complexes of this type as well. The strategy followed in the course of the investigation can be generally recommended for the treatment of dinuclear transition metal complexes.

**Acknowledgment.** We thank the Deutsche Forschungsgemeinschaft and the Fonds der Chemischen Industrie for financial support.

IC9805776